Journal of Bioenergetics and Biomembranes, Vol. 33, No. 1, 2001

A Novel K^+ Channel Expressed in Carrot Roots with a Low Susceptibility Toward Metal Ions

Andrea Paganetto,[1,4] Monica Bregante,[1,4] Patrick Downey,[2] Fiorella Lo Schiavo,[2] Stefan Hoth,[3] Rainer Hedrich,[2] and Franco Gambale[1,5]

Received July 28, 2000; accepted October 5, 2000

Kdc1 is a novel K^+-channel gene cloned from carrot roots, and which is also present in cultured carrot cells. We investigated the characteristics of the ionic current elicited in *Xenopus* oocytes coinjected with KDC1 (K^+-*Daucus carota* 1) and KAT1 (from *Arabidopsis thaliana*) RNA. Expressed heteromeric channels displayed inward-rectifying potassium currents whose kinetics, voltage characteristics, and inhibition by metal ions depended on KDC1:KAT1 ratios. At low KDC1:KAT1 ratios, Zn^{2+} inhibition of heteromeric K^+ current was less pronounced compared to homomeric KAT1 channels, while at higher KDC1:KAT1 ratios, the addition of Zn^{2+} even produced an increase in current. Under the same conditions, the Ni^{2+} inhibition of the current was also reduced, but no current increase was observed. These effects might be explained by the unusual amino acid composition of the KDC1 protein in terms of histidine residues that are absent in the pore region, but abundant (four per subunit) in the proximity of the pore entrance. Channels like KDC1 could be at least partially responsible for the higher resistance of carrot cells in the presence of metals.

KEY WORDS: Ion channels; ionic transport; membranes; metal ions; plants; carrot cells.

INTRODUCTION

Since the patch-clamp technique was first applied to plant cells, K^+-selective channels have been identified in various species and tissues of higher plants. Two major classes of voltage-dependent K^+ channels have been identified: (1) outward rectifiers (such as SKOR; Gaymard *et al.*, 1998) activated by depolarizing membrane potentials, and (2) inward rectifiers that pass inward K^+ fluxes at negative membrane potentials (Maathuis and Sanders, 1999). The biophysical properties of the inward rectifying channels are largely conserved in all plant cells studied. They activate upon hyperpolarization of the plasma membrane, are potassium selective, and blocked by cesium, TEA^+ (Hedrich and Dietrich, 1996), as well as metal ions (Bregante *et al.*, 1997). These basic features are shared by all plant K^+ channel α subunits cloned so far (for review, see Hedrich *et al.*, 1998). With respect to their voltage and pH dependence, however, the α subunits are grouped into two classes. Members of the AKT1 and KAT1 families (*e.g.*, AKT1, SKT1, KAT1, and KST1) only conduct K^+ ions at membrane potentials below the reversal potential for K^+; therefore, they represent strong inward rectifiers (Hoth *et al.*, 1997). By contrast, AKT2-like channels (AKT2/AKT3 and ZMK2) are only weakly regulated by the membrane potential and can also mediate outward K^+ currents (Lacombe *et al.*, 2000; Marten *et al.*, 1999; Philippar *et al.*, 1999). Furthermore, AKT3 and ZMK2 are blocked by protons and, therefore, differ from the acid-activated inward rectifiers. Members of both K^+ channel families are, however, inhibited by TEA^+ and the heavy metal Zn^{2+} (Hoth and Hedrich, 1999a; Ichida and Schroeder, 1996; Hoth and Hedrich, 2000 unpublished). The molecular structure of the K^+ uptake channels

[1] Istituto di Cibernetica e Biofisica-CNR, Via DeMarini 6, 16149, Genova, Italy.
[2] Dipartimento di Biologia, Universitá di Padova, Via Colombo 3, 35121 Padova, Italy.
[3] Julius-von-Sachs Institut fur Biowissenschaften, Lehrstuhl für Molekulare Pflanzen Physiologie und Biophysik, Julius-von-Sachs Platz 2, 97082 Würzburg, Germany.
[4] These authors contributed equally to this study.
[5] To whom all correspondence should be addressed; e-mail: gambale@icb.ge.cnr.it

0145-479X/01/0200-0063$19.50/0

is characterized by six transmembrane segments (S1–S6) and a pore region (P), which harbors the selectivity filter (Doyle *et al.*, 1998; Uozumi *et al.*, 1998). Specific sites for pH regulation, TEA^+ block, and Zn^{2+} binding have been identified by site-directed mutagenesis of the KST1 and KAT1 α subunits. A pore histidine, conserved in all K^+ uptake channels cloned so far, represents the binding site for TEA^+ (Hoth and Hedrich, 1999b). Together with a histidine residue in the S3–S4 linker, this histidine also plays a crucial role in pH sensing and Zn^{2+} binding in KST1 (Hoth *et al.*, 1997; Hoth and Hedrich, 1999a).

Here, we describe the effects mediated by the novel carrot K^+-channel KDC1 (*K*$^+$ *Daucus carota* 1), belonging to the ATKC1 family (Downey *et al.*, 2000), when it is coexpressed with KAT1 in *Xenopus* oocytes. KDC1 lacks the pore histidine, but exposes two pairs of histidines in the S3–S4 and S5–S6 linkers to the external face of the membrane. We wanted to verify whether KDC1 forms heteromeric channels and whether the unusual amino acid composition of KDC1 is able to confer to the heteromeric channel properties significantly different from those of KAT1, namely, a different sensitivity to the heavy metals.

EXPERIMENTAL PROCEDURES

Injection of RNA in Oocytes

Xenopus laevis oocytes were isolated (Hedrich *et al.*, 1995) and injected with KDC1 and KAT1 mRNA (60 ng/μl) using a Drumond "Nanoject" microinjector (25–50 nl/oocyte). RNA concentration was quantified spectroscopically. All the experiments shown were performed using a single batch of the two RNAs (KDC1 and KAT1). However, similar results were also obtained using other KDC1 samples. Current recordings were made 2–6 days after injection. KDC1 and KAT1 (or KAT1 mutants) were simultaneously injected in the desired predetermined weight ratios, *R*, comprised between 0:1 (corresponding to no KDC1) and 2:1. Since some properties of plant K^+ channels may be affected by the expression level, we selected oocytes with comparable K^+-current amplitudes and verified that, under our experimental conditions, oocytes injected with KAT1 and a volume of distilled water identical to that used to coinject KDC1, did not show changes of the KAT1 channel properties (Véry *et al.*, 1994).

Voltage-Clamp Recordings

Whole cell K^+ currents were measured with a two microelectrode home-made voltage-clamp amplifier (designed by F. Conti), using 0.2–0.4 Mohm electrodes filled with 3 M KCl. Unless otherwise indicated, the following bath standard solution was used (in mM): 100 KCl, 2 $MgCl_2$, 1 $CaCl_2$, 10 MES/Tris, pH 5.6. When necessary, ionic solutions were adjusted to 220 mOsm by the addition of sorbitol. Currents were typically filtered with a cut-off frequency of 1 kHz before acquisition. Unless otherwise indicated, each data point represents the mean $\pm$ S.E. obtained from at least three different experiments. The relative open probability was obtained dividing the steady state currents by $(V-V_{rev})$, normalized to the saturation value of the calculated Boltzmann distribution.

Molecular Biology

Kdc1 was amplified from carrot root cDNA using an RT-PCR strategy (Downey *et al.*, 2000). The coding sequence was cloned as a blunt-ended (sense orientation) fragment into the *Sma*I site of vector pGEMHE (Liman *et al.*, 1992). To provide a linear template for *in vitro* transcription, pGEMHE-KDC1 was digested with *Sph*I, which cuts after the 3′ UTR of the *Xenopus* β–globin gene. Linearized DNA was purified and dissolved in RNase-free water. The mCAP mRNA kit (Stratagene) was used to synthesize sense-strand RNA. The RNA was quantified by optical density at 260 nm and visualized on an acrylamide gel.

Cell Cultures

Carrot (*Daucus carota* cv. "S.Valery") and *Arabidopsis (Arabidopsis thaliana*, ecotype Landsberg) suspension cells were cultured in B5 Gamborg's medium (Flow) supplemented with 0.5 mg/l (2.3 μM) 2-4,D, and 0.25 mg/l (0.11 μM) 6-BAP (benzoaminopurine). Cells in the exponential phase, 3 days after the transfer to fresh medium, were filtered through a nylon screen of 200-μm pore size, counted, and plated in the B5 solid medium at 4×10^3 cell units/ml. Ten days later, the colonies were counted to determine the plating efficiency.

RESULTS

In order to verify whether KDC1 displays peculiar sensitivity to metal ions, we choose *Xenopus* oocytes as an expression system for *Kdc1* cRNA. Unfortunately, oocytes injected with KDC1 alone did not exhibit any K^+ channel activity (Fig. 1a) at membrane potentials between $+100$ and -160 mV. Increasing the concentration of KDC1-cRNA, as an example, up to 10 times that typically injected

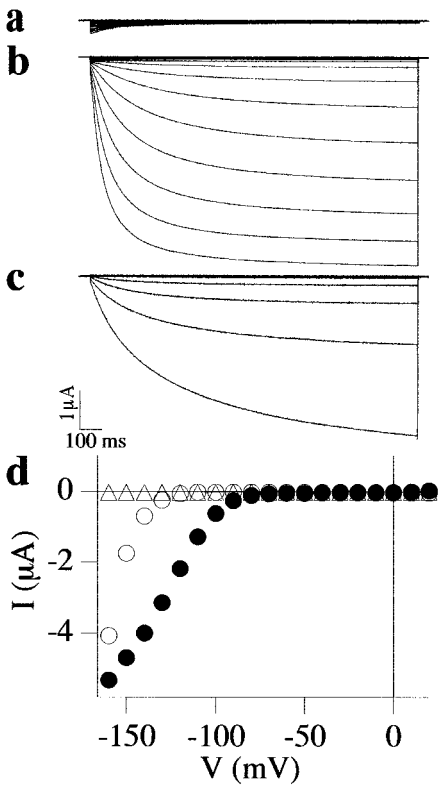

Fig. 1. Functional expression of KDC1, KAT1, and KDC1:KAT1 mixtures in oocytes. Ionic currents elicited by voltage steps from −160 to +20 mV in 10-mV increments from a holding potential of 0 mV, in oocytes injected with (a) KDC1, (b) KAT1, and (c) coinjected with KDC1: KAT1 at a weight ratio, *R*, equal to 1:1. (d) Current voltage characteristics of the family currents shown in (a–c), obtained by plotting the mean value of the last 60 ms as a function of the applied voltage. KDC1 (△); KAT1 (●); KDC1:KAT1=1:1 (o).

to elicit KAT1 currents, failed to elicit KDC1 currents. Also, variations of various physicochemical parameters like internal and external pH, temperature, concentration of ionic solutions, and MgATP did not favor the appearance of pure ionic currents mediated by the KDC1 channel.

On the other hand, K^+-channel subunits aggregate in expression systems to form heteromultimeric channels displaying properties that depend on the characteristics of the *n*-mers assembled (Dreyer *et al.*, 1997). Therefore, we decided to verify whether KDC1 is involved in the modulation of ionic currents when coinjected with other potassium channels. We selected KAT1 to support the coexpression of KDC1 because its properties in oocytes have been intensively investigated and the coassembly of heteromeric oligomers is neither plant- nor tissue-specific.

Consistently with evidences of other authors that adopted oocyte coexpression as a model system for the characterization of plant and animal multimeric channels (Baizabal-Aguirre *et al.*, 1999; Dreyer *et al.*, 1997; Lee *et al.*, 1994; Lynch *et al.*, 1999), KDC1:KAT1 coexpression products also displayed inward currents, which differed significantly from currents mediated by KAT1 homomers. In oocytes coinjected with identical amounts of KDC1 and KAT1 (R = 1:1), currents displayed much slower activation kinetics (Figs. 1c and 2a) and activated at more negative membrane potentials (Figs. 1d and 2c) when compared to KAT1 currents. The currents shown in Fig. 1c clearly cannot be generated by the independent tetramerization of two homomeric entities (KDC1 and KAT1). They are mediated by heteromers, where KDC1 changes the characteristics of the KAT1 channel. This was confirmed by experiments showing that the slower kinetics of the heteromeric currents strongly correlated with the percentage of KDC1 coinjected. In Fig. 2, the variation of the time constants of current activation (panel a, at $V = -150$ mV) and deactivation (b, to $V = -80$ mV) and the shift (panel c) of the open-probability characteristics are plotted as a function of the KDC1 fraction. The activation and deactivation times of the heteromeric currents resembled the voltage dependence of the KAT1 currents (not shown; see Hedrich *et al.*, 1995); however, with respect to KAT1, increasing the KDC1 concentration (from R = 0:1 to 2:1) slowed the kinetics of current activation [$t_{1/2}$(KAT1) = 103 ± 2 ms, $n = 3$] and deactivation [τ(KAT1) = 86 ± 13 ms, $n = 4$] 2.5 times, shifted the half-maximal activation potential $V_{1/2}$ by −45 mV [$V_{1/2}$(KAT1) = −127 ± 1 mV], and (up to R = 1:1) increased the apparent gating valence (see Fig. 2).

Like KAT1, the heteromeric channels were potassium-selective. Tail currents obtained at different external potassium concentrations demonstrated that the reversal potential is in agreement (Fig. 3a) with the theoretical Nernst potentials for K^+. Figure 3b summarizes the variations of the reversal potential obtained at potassium concentrations that ranged between 3 and 100 mM at R = 1:2. Similar results were also obtained at other KDC1:KAT1 weight ratios.

In line with KAT1 homomers, the heteromeric channels were blocked by submillimolar concentrations of external cesium. The typical decrease of the KAT1 current upon the addition of 0.2 mM Cs^+ (Fig. 4a) could also be observed for KDC1:KAT1 mixtures (Fig. 4b). As an example, Fig. 4c demonstrates the similar blocking characteristics of KAT1 and heteromers (R = 1:1).

In contrast to Cs^+ block, heteromeric KDC1:KAT1 channels displayed a lower sensitivity to tetraethylammonium (TEA). While KAT1 currents decreased by about 50% upon the addition of 1 mM TEA^+ (Fig. 4d), KDC1:KAT1 channels (R = 1:1) were only slightly blocked by 1 mM TEA^+ (Fig. 4e). The K_m for TEA

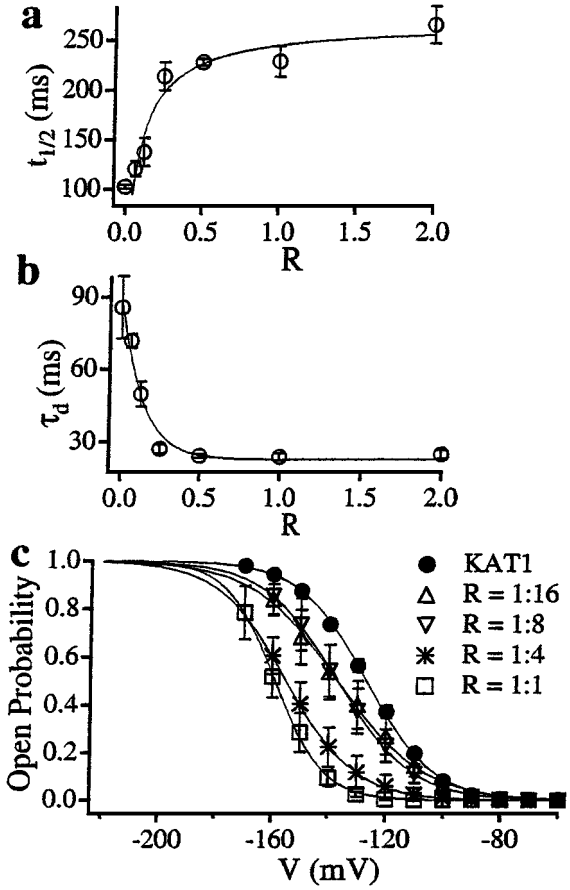

Fig. 2. KDC1 coinjected with KAT1 alters the kinetics and activation characteristics of the inward currents. (a) The half-activation times of ionic currents elicited in response to voltage steps to −150 mV are plotted as a function of *R*. Data points were fitted by a Michaelis–Menten curve with a $K_m = 0.09 \pm 0.01$ (mean ± S.D.). (b) Current deactivation-time constants, τ_d, plotted as a function of *R*. τ_d were obtained from monoexponential fit of tail currents to −80 mV, following a conditioning prepulse to −150 mV. The continuous line represents the exponential fit to the data points. (c) Typical open-probability characteristics of the heteromeric inward channel recorded in oocytes injected with different KDC1:KAT1 ratios. The probability characteristics were obtained plotting (as a function of the applied potential) the normalized steady-state conductance obtained from families of ionic currents, like those shown in Fig. 1. The best fit of the open probability gave the following values for the half-activation potentials, $V_{1/2}$, and apparent gating valence, *z* (*n* = number of experiments): KAT1 (-127 ± 1 mV, $z = 1.6 \pm 0.1$, $n = 3$), $R_{1:16}$ (-137 ± 2 mV, $z = 1.7 \pm 0.1$, $n = 6$), $R_{1:8}$ (-137 ± 1 mV, $z = 1.9 \pm 0.1$, $n = 15$), $R_{1:4}$ (-155 ± 1 mV, $z = 2.1 \pm 0.1$, $n = 11$), $R_{1:2}$ (-161 ± 2 mV, $z = 2.4 \pm 0.1$, $n = 8$), $R_{1:1}$ (-159 ± 1 mV, $z = 2.9 \pm 0.1$, $n = 8$), $R_{2:1}$ (-172 ± 1 mV, $z = 1.3 \pm 0.1$). For clarity reasons, only the characteristics at $R = 1{:}16$, 1:8, 1:4, and 1:1 are shown.

inhibition changed from (0.9 ± 0.1) mM for KAT1 to (2.8 ± 0.3) mM for KDC1:KAT1 = 1:4 (see Fig. 4f).

The most obvious characteristic of the heteromeric channels was the different sensitivity to external metal ions. Whereas KAT1 was significantly blocked by the

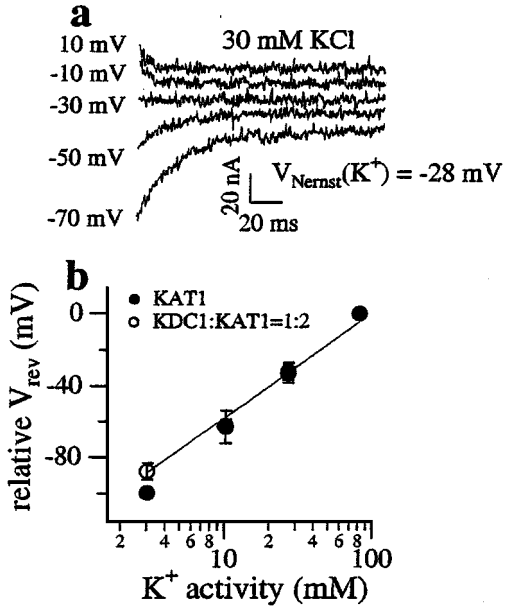

Fig. 3. The heteromeric channel is potassium-selective. KDC1 coinjected with KAT1 ($R = 1{:}2$) did not affect the reversal potential of the inward currents. (a) Representative tail currents, following the ionic current elicited by double-voltage pulses in 30 mM KCl. After hyperpolarization to −150 mV, currents relax to new steady states upon subsequent steps to depolarizing potentials. (b) The reversal potential derived from instantaneous tail currents was plotted as a function of the external K^+ activity in oocytes injected with KAT1 alone and KDC1:KAT1 = 1:2. The continuous straight line represents a shift of the reversal potential by 59 mV for a tenfold change in the K^+concentration. Each data point was derived from 3 to 7 experiments.

addition of 5 mM Zn^{2+} to the bath solution (Figs. 5a and c), Zn^{2+} inhibition of the heteromeric currents (at R = 1:8 and 1:16) was less pronounced (Fig. 5c). Surprisingly, when *R* was raised above 1:8, the addition of external Zn^{2+} resulted in an increase in the normalized current that is particularly notable (up to fourfold) at large *R* (Fig. 5b–d). Specifically, on addition of Zn^{2+}, the ionic current increases with the KDC1:KAT1 ratio, as documented in Fig. 5d, where $I_{Zn}/I_{control}$, measured in the presence of 5 mM Zn^{2+}, is plotted as a function of *R*. It can be observed that also the absolute value of the heteromeric current can be greater than that of KAT1 under the same conditions (see Fig. 5b).

The increase in the macroscopic conductance induced by Zn^{2+} on the heteromeric channel ($R = 1{:}1$), compared to the decrease of the KAT1 conductance, is illustrated in Fig. 6a. In panel (b) it can be observed that on the addition of Zn^{2+}, the opening-probability characteristics of the KAT1 channel did not change appreciably, while the characteristics of the heteromeric channel displayed a significant modification of the voltage sensitivity with a partial "recovery" of the apparent valence (z)

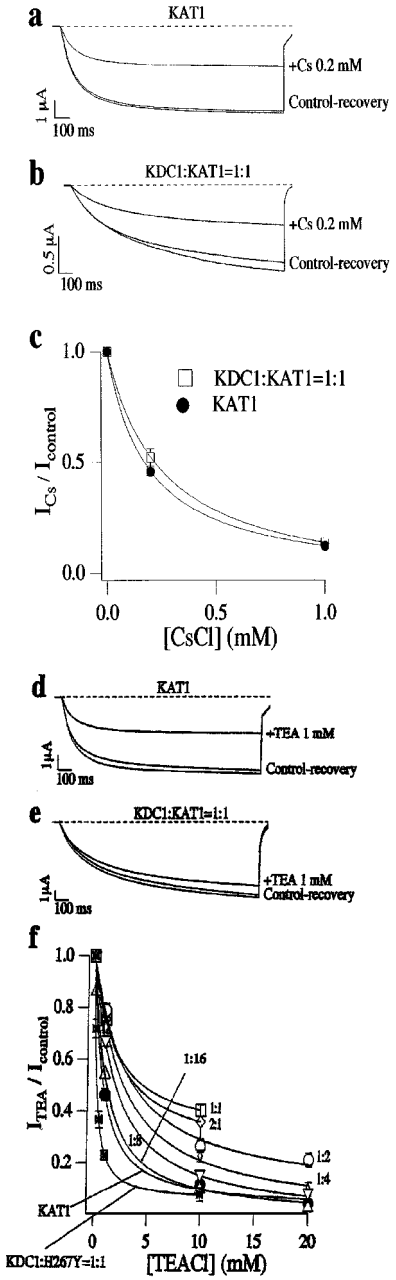

Fig. 4. The heteromeric channel is reversibly blocked by external cesium and TEA. Typical ionic currents recorded in oocytes injected with KAT1 alone before (control) and after (recovery) the removal of 0.2 mM Cs^+ (panel a) and 1 mM TEA^+ (panel d) from the bath solution. Inhibition of heteromeric ($R = 1{:}1$) currents on the addition of 0.2 mM Cs^+ (b) and 1 mM TEA^+ (e). Panels (c) and (f) show cesium and TEA^+ inhibitory dose response for oocytes injected with KAT1 and KDC1:KAT1=1:1. Data obtained from at least three different experiments; applied transmembrane potential −150 mV. Continuous line represents exponential fit to the experimental data. Increasing the percentage of KDC1 in the composition of heteromeric channels determined a decreased blocking by TEA^+. $I_{TEA}/I_{control}$ and $I_{Cs}/I_{control}$ (plotted as a function of TEA^+ and Cs^+ concentration) represents the normalized steady-state current elicited in the presence of TEA^+ and Cs^+ by membrane voltages to −150 mV. Numbers close to each curve indicate the corresponding subunit ratio, *R*.

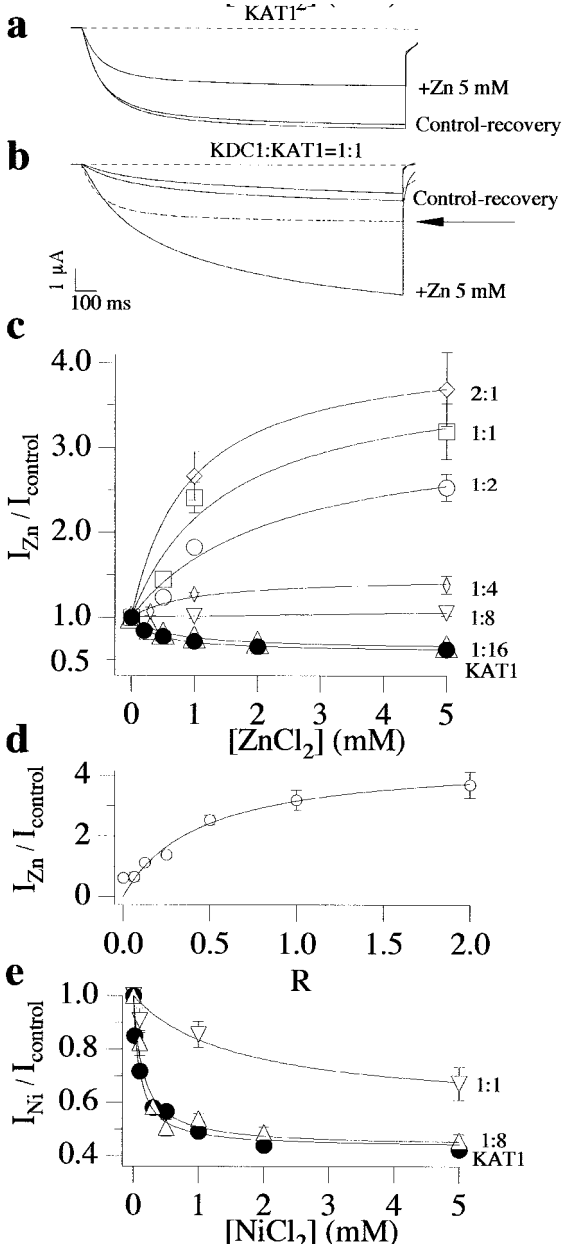

Fig. 5. Heteromeric KDC1:KAT1 channels display a modified sensitivity to Zn^{2+} and Ni^{2+}. (a) Cytoplasmic Zn^{2+} typically blocked up to 50% of the KAT1 current. An increase in KDC1 percentage determined a progressively lower Zn^{2+} block of the current at $R \leq 1{:}8$; conversely, at large *R* (>1:8), the addition of Zn^{2+} resulted in a marked increase in the current. See, for example, panel (b), where the heteromeric currents are compared with the dashed curve (indicated by the arrow) representing the KAT1 current in the presence of Zn^{2+}. (c) $I_{Zn}/I_{control}$ represent the steady state of the ionic current recorded in the presence of Zn^{2+} with respect to the control (*i.e.*, $Zn^{2+} = 0$). (d) $I_{Zn}/I_{control}$ measured in the presence of 5 mM Zn^{2+} is plotted as a function of *R*. (e) With respect to homomultimeric KAT1 channels, the heteromeric channels also show a lower sensitivity to the blocking action induced by Ni^{2+} added to the bath solution. In panels (c) and (e), the numbers close to each curve indicate the corresponding subunit ratio, *R*. Applied transmembrane potentials to −150 mV.

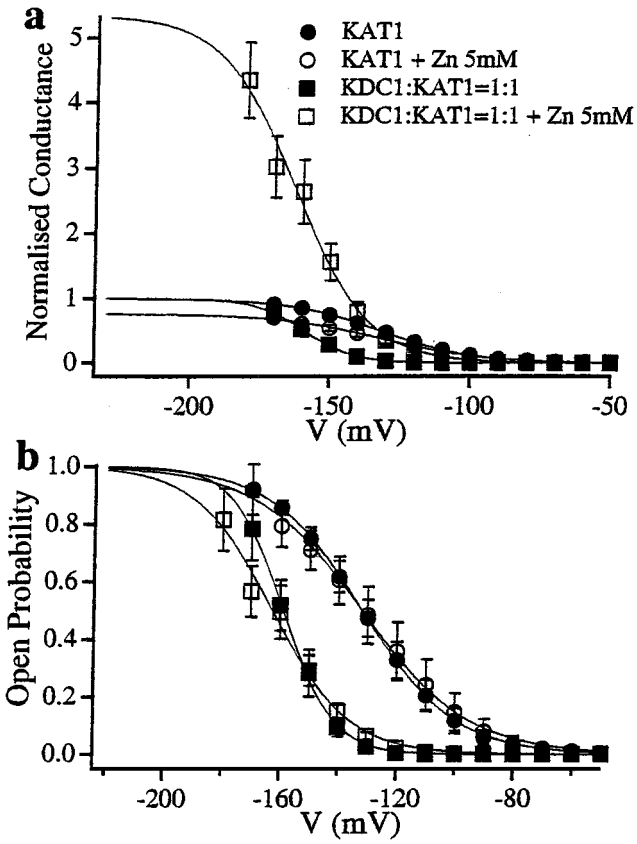

Fig. 6. Zn^{2+} affects the opening probability of the heteromeric channel. (a) Decrease (empty circles) and increase (empty squares) in the macroscopic conductance of KAT1 and heteromeric ($R = 1{:}1$) channels upon addition of Zn^{2+} (5 mM). Data were normalized with respect to respective control (*i.e.*, KAT1, filled circles) and heteromers (filled squares). (b) Comparison of the open probability of curves shown in (a).

toward the values measured in KAT1 channels. The best fit of the opening probability with the Boltzmann distribution $P = 1/[1+ \exp(zF(V - V_{1/2})/RT]$ gave the following values for z and the half-activation potentials ($V_{1/2}$): KAT1(control) $z = 1.6 \pm 0.1$, $V_{1/2} = (-132 \pm 1)$ mV; KAT1($+Zn^{2+} = 5$ mM) $z = 1.4 \pm 0.1$, $V_{1/2} = (-132 \pm 1)$ mV; KDC1:KAT1(control) $z = 2.9 \pm 0.1$, $V_{1/2} = (-159 \pm 1)$ mV; KDC1:KAT1 ($+Zn^{2+} = 5$ mM) $z = 1.9 \pm 0.2$, $V_{1/2} = (-163 \pm 1)$ mV (each data point was obtained from 3 to 8 experiments). A similar trend, indicating a decrease of z, was also observed on the addition of lower zinc concentration at $R = 1{:}2$.

In order to verify the specificity of Zn^{2+} action on the hetero-multimeric channel, we compared Zn^{2+} effects with those induced by Ni^{2+} (Fig. 5e). We never observed any increase in the ionic current with any KDC1:KAT1 ratio, even at large (up to 5 mM) Ni^{2+} concentration. At low $R \leq 1{:}8$, the effect induced by Ni^{2+} on the heteromultimeric channel did not significantly differ from

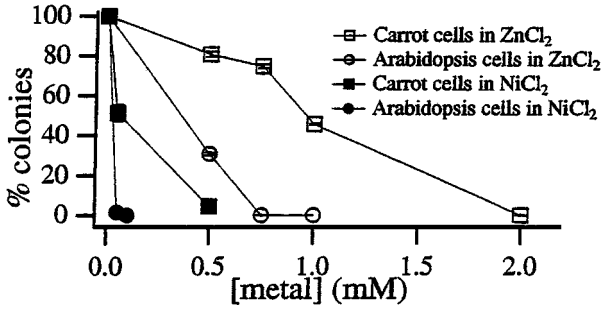

Fig. 7. Toxicity curves of zinc and nickel. Plating efficiency represented by the normalized number of colonies/petri dish of *D. carota* and *A. thaliana* cells cultured in growing medium in the presence of different concentrations of $ZnCl_2$ and $NiCl_2$. SE are smaller than the symbols.

those induced in homomeric KAT1 channel. Only oocytes injected with relatively high KDC1:KAT1 ratios ($R \geq 1{:}2$) displayed an inhibition of the heteromeric current, which was consistently lower than that observed in homomeric KAT1 channels.

Kdc1 was cloned from carrot roots. However, RT-PCR experiments demonstrated that the channel is also expressed in A^+t3 cultured carrot cells obtained from carrot hypocotyls (Downey *et al.*, 2000). For this reason, we decided to verify whether cultured carrot cells, grown in the presence of $ZnCl_2$ and $NiCl_2$, are more tolerant to these metal ions than *A. thaliana* cell cultures, chosen as a control system. This was verified by evaluating the plating efficiency of cultured cells in the presence of different concentrations of zinc and nickel. In the presence of either of the two metals, carrot colonies reduced to 50% of plated cells at concentrations at least two times greater than the corresponding value characterizing *A. thaliana* cultures grown under identical conditions (Fig. 7).

DISCUSSION

Kdc1, cloned from *Daucus carota* root cDNA, encodes a 72.3 KDa protein (629 AA), highly homologous to other inward K^+ channel identified in other plants and tissues (Downey *et al.*, 2000). KDC1 channel is also expressed in carrot cell cultures, as shown by Downey *et al.*, (unpublished results); also, patch-clamp experiments performed on protoplasts obtained from cultured carrot cells (Bregante *et al.*, 1996) and root hairs (Downey *et al.*, 2000) display inward currents with characteristics typical of inward potassium channels, such as potassium selectivity, voltage-dependent activation, blockage by external cesium, high negative threshold of activation (up to -150 at neutral pH), and slow kinetics of activation ($t_{1/2} \geq 100$ ms at $V = -160$ mV) (Bregante *et al.*, 1996). Here, we demonstrate that carrot KDC1, coexpressed in *Xenopus*

oocytes together with the *Arabidopsis* KAT1 channel, has a role in sustaining ionic currents showing properties significantly different from those mediated by homomeric KAT1 channels. We suggest that these modifications of KAT1 currents are due to the formation of heteromeric KDC1:KAT1 channels and not to the action of oocyte modulatory components elicited by KDC1. Indeed, increasing percentages of KDC1 elicit inward-rectifying currents that exhibit progressively slower kinetics of activation, faster current deactivation, and a threshold of activation shifted toward negative voltages. These properties are reminiscent of the slow activation kinetics and the very negative activation threshold of the inward channels measured in carrot cell protoplasts (Bregante *et al.*, 1996). The fact that the heteromeric channels are selectively permeable to K^+ and reversibly blocked by cesium indicates that the size of the selectivity filter is unchanged with respect to the KAT1 channel. This is not surprising, since the relevant change in the pore region of KDC1 is in position 269 (*i.e.*, 264GYGDLY), where a tyrosine group substitutes for the typical histidine residue present in all other plant K^+ channels (Hoth *et al.*, 1997). This change is located relatively far from the K^+ channel selectivity filter (Doyle *et al.*, 1998), but proximal to the region that influences the TEA blockade (Heginbotham and MacKinnon, 1992; Yellen *et al.*, 1991). Indeed, in plant inward K^+ channels, the histidine in the pore region regulates the binding of TEA^+, as demonstrated by the lower blockage observed in KST1-H271A and KAT1-H267A mutants (Hoth and Hedrich, 1999b). Therefore, the lower sensitivity to TEA^+ of the current measured in coinjected oocytes is consistent with the presence of Y269 in KDC1 and support the hypothesis that the conducting channel is formed by KDC1:KAT1 heteromers. This is only apparently in contradiction with the higher affinity observed, as an example, in *Shaker* K^+ channels, where threonine-469 in the pore region was replaced by a tyrosine (Heginbotham and MacKinnon, 1992). In fact, the symmetry provided by the presence of two or four imidazole groups seems to be essential for high affinity (Heginbotham and MacKinnon, 1992) TEA^+ binding. For obvious reasons, these symmetry conditions, which are always achieved in homomeric K^+ channels obtained by the expression of a single subunit, are present only in a small fraction of the heteromultimeric channels (Naranjo, 1997) in our working conditions. This hypothesis is confirmed by other experiments where KDC1 was coinjected together with the KAT1 mutant KAT1-H267Y; this heteromer (KDC1:KAT1-H267Y = 1:1), that obviously brings four tyrosines in the pore, has an affinity for TEA^+ (empty butterfly in Fig. 4f), which is even higher than that displayed by the multihomomeric KAT1 channel (filled circles in Fig. 4). This observation is in accordance with the symmetry requirement of the imidazole groups (Heginbotham and MacKinnon, 1992) and strengthen the hypothesis that the modified current properties depend on the formation of heteromultimeric channels of KDC1 and KAT1 and not on indirect modulation of unknown oocyte components activated by KDC1.

With respect to the effects of Zn^{2+} and Ni^{2+}, heteromeric channels showed an unusual sensitivity to the action of these two metal ions. Heteromers apparently displayed a much lower sensitivity to block by Zn^{2+} and Ni^{2+}. Furthermore, while on the addition of Ni^{2+} the presence of KDC1 never produced any increase in the heteromeric current, at large percentages of KDC1 ($R > 1{:}8$), Zn^{2+} consistently increased the inward current (see Fig. 5d). Since the imidazole ring of histidine is nucleophilic for Zn^{2+} and KDC1 is characterized by a peculiar amino acid composition in terms of histidine residues, it is tempting to speculate that these peculiar properties may be ascribed to the presence of KDC1 in the heteromeric complex. Indeed, it must be observed that, beside the mutation in the pore region, KDC1 differs from other plant K^+ channels because it possesses two pairs of histidines at the linkers connecting α-helix S3–S4 (H161–H162) and α-helix S5–S6, namely, in the S5–P loop (H224–H225) (Downey *et al.*, 2000). No other plant K^+ channel displays such a high concentration of histidine residues facing the external bath solution. It should be noted that the two histidine pairs are located very close to the α-helices S4 and S5, respectively, and, therefore, in close proximity of the voltage sensor and the pore entrance. Moreover, it has been suggested that the surface charges of the S5-P loop play a relevant functional role in the gating properties of the K^+ voltage-dependent channels (Elinder and Århem, 1999; Elinder *et al.*, 1996).

Therefore, we suggest that the absence of the histidine in the pore region and the presence of the extraplasmatic histidines are responsible for the modulation of the current through the heteromeric channels by two distinct mechanisms: (1) Y269 may be responsible for reducing the inhibition of the current, because of the channel block by Zn^{2+} and Ni^{2+}, while (2) the histidines exposed toward the bath solution may be responsible for the increase in the current, for example, because of a modification of the surface charges and/or channel-gating mechanisms. The prevalence of one or the other mechanism may result in a lower inhibition or an increase in the heteromeric current. As an example, the decrease of the channel blocking may prevail at small *R*, while the binding of the metals to external histidines may predominate at large *R*.

The first mechanism (1) is consistent with the reduced sensitivity to Zn^{2+}, which is also demonstrated

in the KST1 channel mutant KST1-H271A where the histidine of the pore region was mutated into alanine (Hoth and Hedrich, 1999a). We have also performed control experiments with the KAT1-mutant H267Y (corresponding to Y269 of KDC1) in which the pore histidine was changed into a tyrosine. Consistently, on the addition of 1 mM Zn^{2+}, the percentage of the steady-state current blocking revealed a decreased inhibition of the KAT1-H267Y current ($1.7 \pm 0.9\%$, $n = 3$) compared to wild-type KAT1 ($15.1 \pm 3.3\%$, $n = 3$), but no current increase was observed. The second mechanism (2) is consistent with the slight variations of the voltage sensitivity of the heteromeric characteristics (reported in Fig. 6); Zn^{2+} possibly modifies the channel-gating characteristics (Elinder and Århem, 1999; Elinder *et al.*, 1996; Schoppa *et al.*, 1992) by short-distance interaction with the KDC1 external histidine imidazole rings. Other mechanisms, such as surface charge effects and steric modifications may participate in increasing the ionic current in the presence of Zn^{2+} (shown in Figs. 5b–d and 6a), for example, by means of an increase in the K^+ concentration at the channel mouth or by an increase in the single-channel conductance. In these mechanisms, a zinc-mediated coordination of the histidines residing on the two linkers (S3–S4 and S5–S6) cannot be excluded. Consistent with this hypothesis, KAT1 I-V characteristic was little affected by Zn^{2+} (Chakrabarti, 1990).

We also verified that the increase in the current induced by Zn^{2+} was not due to an increase in any oocyte endogenous chloride current (Ackerman *et al.*, 1994; Chao and Katayama, 1991; Machaca and Hartzell, 1998) because we systematically selected oocytes that did not display any endogenous inward current, while in noninjected control oocytes, the endogenous currents were inhibited by the addition of Zn^{2+}. The lower percentage of inhibition (with respect to KAT1) of the heteromeric current upon addition of Ni^{2+} can be explained by the fact that while histidine residues primarily bind Zn^{2+}, they also show high affinity for other metal ions (like Ni^{2+} and Co^{2+}) (Krämer *et al.*, 1996; Smith and Martell, 1989). On the other hand, this affinity may not be sufficient to elicit the increase in the current by Ni^{2+} at the KDC1:KAT1 ratios used in this study.

We chose KAT1 to favor the coexpression of KDC1, as KAT1 is a reliable channel whose properties in *Xenopus* oocytes are well characterized and because it has already been suggested (Dreyer *et al.*, 1997) that the coassembly of heteromeric oligomers is neither plant- nor tissue-specific. Indeed, KDC1 and KAT1 belong to two different inward-rectifying channel subfamilies: KAT1 from *A. thaliana* is predominantly expressed in guard cells, while KDC1 from *D. carota* (which belongs to ATKC1 subfamily) is expressed in roots (Downey *et al.*, 2000). It must also be observed that, since another putative K^+ channel seems to be expressed in carrot roots (Downey, 2000 personal communication), the formation of heteromeric channels (formed by this second subunit and KDC1) can be hypothesized in carrot roots.

Despite the fact that other mechanisms, different from KDC1, may be responsible for the metal resistance observed in cultured carrot cells and seeds, we suggest that the insertion of metal-resistant K^+ channels (like KDC1) in other plants could help these plants to grow on metal rich-soils. In this perspective, studies performed on *Xenopus* oocytes have proved to be of crucial importance, because this system allows the coinjection of different clones at reliable predetermined ratios, providing information on potential effects of KDC1 in combination with other plant K^+ channels. Extension of these studies to plant channels cloned from other tissues (*e.g.*, *Arabidopsis* root) and side-directed mutagenesis of specific KDC1 amino acids will allow us to further clarify the mechanisms, providing KDC1 with the peculiar properties illustrated in this paper.

ACKNOWLEDGMENTS

The helpful collaboration of A. Carpaneto and A. Naso was greatly appreciated. This work was supported by special research grants from the Target Project "Progetto Finalizzato Biotecnologie, Sub-project Biotecnologie Ambientali, CNR" and Progetto Finalizzato MIPAF, Italy.

REFERENCES

Ackerman, M. J., Wickman, K. D., and Clapham, D. E. (1994). *J. Gen. Physiol.*, pp. 153–179.

Baizabal-Aguirre, V. M., Clemens, S., Uozumi, N., and Schroeder, J. I. (1999). *J. Membr. Biol.* **167**, 119–125.

Bregante, M., Gambale, F., and LoSchiavo, F. (1996). *FEBS Lett.* **380**, 97–102.

Bregante, M., Carpaneto, A., Pastorino, F., and Gambale, F. (1997). *Eur. Biophys. J.* **26**, 381–391.

Chakrabarti, P. (1990). *Protein. Eng.* **4**, 57–63.

Chao, A. C. and Katayama, Y. (1991). *Biochem. Biophys. Res. Commun.* **180**, 1377–1382.

Doyle, D. A., Cabral, J. M., Pfuetzner, R. A., Kuo, A., Gulbis, J. M., Cohen, S., Chait, B. T., and MacKinnon, R. (1998). *Science* **280**, 69–77.

Downey, P., Szabò, I., Hedrich, R., Terzi, M., and Lo Schiavo, F. (2000). *J. Biol. Chem.* **275**, 39420–39426.

Dreyer, I., Antunes, S., Hoshi, T., Müller-Röber, B., Palme, K., Pongs, O., Reintanz, B., and Hedrich, R. (1997). *Biophys. J.* **72**, 2143–2150.

Elinder, F. and Århem, P. (1999). *Biophys. J.* **77**, 1358–1362.

Elinder, F., Madeja, M., and Århem, P. (1996). *J. Gen. Physiol.* **108**, 325–332.

Gaymard, F., Pilot, G., Lacombe, B., Bouchez, D., Bruneau, D., Boucherez, J., Michaux-Ferriere, N., Thibaud, J. B., and Sentenac, H. (1998). *Cell* **94**, 647–655.

Hedrich, R., Moran, O., Conti, F., Bush, H., Becker, D., Gambale, F., Dreyer, I., Kuch, A., Neuwinger, K., and Palme, K. (1995). *Eur. Biophys. J.* **24**, 107–115.

Hedrich, R. and Dietrich, P. (1996). *Botan. Acta* **109**, 1–8.

Hedrich, R., Hoth, S., Dreyer, I., Becker, D., and Dietrich, P. (1998). In *Cellular integration of signalling pathways in plant development* NATO ASI Series, v. H104, (Lo Schiavo, F., Last, R. L., Morelli, G., Raikhel, N. V. eds.) Springer-Verlag, Berlin and Heidelberg, pp. 35–45.

Heginbotham, L. and MacKinnon, R. (1992). *Neuron* **8**, 483–491.

Hoth, S., Dreyer, I., Dietrich, P., Becker, D., Müller-Röber, B., and Hedrich, R. (1997). *Proc. Natl. Acad. Sci. USA* **94**, 4806–4810.

Hoth, S. and Hedrich, R. (1999b). *J. Biol. Chem.* **274**, 11599–11603.

Hoth, S. and Hedrich, R. (1999a). *Planta* **209**, 543–546.

Ichida, A. M. and Schroeder, J. I. (1996). *J. Membr. Biol.* **151**, 53–62.

Krämer, U., Cotten-Howells, J. D., Charnock, J. M., Baker, A. J. M., and Smith, J. A. C. (1996). *Nature* (*London*) **379**, 635–638.

Lacombe, B., Pilot, G., Michard, E., Gaymard, F., Sentenac, H., and Thibaud, J. B. (2000). *Plant Cell* **12**, 837–851.

Lee, T. E., Philipson, L. H., Kuznetsov, A., and Nelson, D. J. (1994). *Biophys. J.* **66**, 667–673.

Liman, E. R., Tytgat, J., and Hess, P. (1992). *Neuron* **9**, 861–871.

Lynch, P. J., Tong, J., Lehane, M., Mallet, A., Giblin, L., Heffron, J. J. A., Vaughan, P., Zafra, G., MacLennan, D. H., and McCarthy, T. V. (1999). *Proc. Natl. Acad. Sci. USA* **96**, 4164–4169.

Maathuis, F. J. M. and Sanders, D. (1999). *Curr. Opin. Plant Biol.* **2**, 236–246.

Machaca, K. and Hartzell, H. C. (1998). *Biophys. J.* **74**, 1286–1295.

Marten, I., Hoth, S., Deeken, R., Ache, P., Ketchum, K. A., Hoshi, T., and Hedrich, R. (1999). *Proc. Natl. Acad. Sci. USA* **96**, 7581–7586.

Naranjo, D. (1997). In *From ion channel to cell-to-cell conversation*, (Latorre, R. and Sàez, J. C. eds) Plenum Press, New York and London, pp. 35–65.

Philippar, K., Fuchs, I., Lüthen, H., Hoth, S., Bauer, C., Haga, K., Thiel, G., Ljung, K., Sandberg, G., Böttger, M., Becker, D., and Hedrich, R. (1999). *Proc. Natl. Acad. Sci. USA* **96**, 12186–12191.

Schoppa, N. E., McCormack, K., Tanouye, M. A., and Sigworth, F. J. (1992). *Science* **255**, 1712–1715.

Smith, R. and Martell, A. E. (1989). *Critical stability constants* v. 6, Plenum Press, New York.

Uozumi, N., Nakamura, T., Schroeder, J. I., and Muto, S. (1998). *Proc. Natl. Acad. Sci. USA* **95**, 9773–9778.

Véry, A. A., Bosseux, C., Gaymard, F., Sentenac, H., and Thibaud, J. B. (1994). *Pflügers Arch.* **428**, 422–424.

Yellen, G., Jurman, M. E., Abramson, T., and MacKinnon, R. (1991). *Science* **251**, 939–942.